Inorg. Chem. **2002**, *41*, 1281–1291

Synthesis, Characterization, Electrochemistry, Electronic Structure, and Isomerization of Mononuclear Oxo–Molybdenum(V) Complexes: The Serine Gate Hypothesis in the Function of DMSO Reductases

Brian Kail,[†] Victor N. Nemykin,[†] Scott R. Davie,[†] Carl J. Carrano,[‡] Brian Hammes,[‡] and Partha Basu*,[†]

Department of Chemistry and Biochemistry, Duquesne University, Pittsburgh, Pennsylvania 15282, and Department of Chemistry and Biochemistry, Southwest Texas State University, San Marcos, Texas 78666

Received November 15, 2001

Crystal structures of DMSO reductases isolated from two different sources and the crystal structure of related trimethylamine-*N*-oxide reductase indicate that the angle between the terminal oxo atom on the molybdenum and the serinato oxygen varies significantly. To understand the significance of this angular variation, we have synthesized two isomeric compounds of the heteroscorpionato ligand (L1OH) (*cis*- and *trans*-(L1O)$Mo^{V}OCl_2$), where the phenolic oxygen mimics the serinato oxygen donor. Density functional and semiempirical calculations indicate that the trans isomer is more stable than the cis. The lower stability of the cis isomer can be attributed to two factors. First, a strong antibonding interaction between the phenolic oxygen with molybdenum d_{xy} orbital raises the energy of this orbital. Second, the strong trans influence of the terminal oxo group in the trans isomer places the phenol ring, and hence the bulky tertiary butyl group, in a less sterically hindered position. In solution, the cis isomer spontaneously converts to the thermodynamically favorable trans isomer. This geometric transformation follows a first-order process, with an enthalpy of activation of 20 kcal/mol and an entropy of activation of –9 cal/mol K. Computational analysis at the semiempirical level supports a twist mechanism as the most favorable pathway for the geometric transformation. The twist mechanism is further supported by detailed mass spectral data collected in the presence of excess tetraalkylammonium salts. Both the cis and trans isomers exhibit well-defined one-electron couples due to the reduction of molybdenum(V) to molybdenum(IV), with the cis isomer being more difficult to reduce. Both isomers also exhibit oxidative couples because of the oxidation of molybdenum(V) to molybdenum(VI), with the cis isomer being easier to oxidize. This electrochemical behavior is consistent with a higher-energy redox orbital in the cis isomer, which has been observed computationally. Collectively, this investigation demonstrates that by changing the O_t–Mo–O_p angle, the reduction potential can be modulated. This geometrically controlled modulation may play a gating role in the electron-transfer process during the regeneration steps in the catalytic cycle.

Introduction

Dimethyl sulfoxide reductase (DMSO reductase) is a pyranopterin-bound mononuclear molybdenum enzyme that catalyzes the reduction of dimethyl sulfoxide (DMSO) to dimethyl sulfide (DMS).[1−4] This reductive process is important in the biogenic sulfur cycle and has been implicated to play critical roles in cloud formation and global temperature control.[5] Unlike the majority of the mononuclear molybdenum enzymes, DMSO reductases from *Rhodobacter spheroides* and *R. capsulatus* have the molybdenum center as the sole prosthetic group.[1] The absence of other prosthetic groups has allowed detailed spectroscopic investigations to probe the active site directly. Thus, DMSO reductases have been investigated by extended X-ray absorption fine structure

* Corresponding author. E-mail: basu@duq.edu.
[†] Duquesne University.
[‡] Southwest Texas State University.

(1) Hille, R. *Chem Rev.* **1996**, *96*, 2757.
(2) Pilato, R. S.; Stiefel, E. I. In *Inorganic Catalysis*, 2nd ed.; Reedijk, J., Bouwman, E., Eds.; Marcel Dekker: New York, 1999; pp 81−152.
(3) Enemark, J. H.; Young, C. G. *Adv. Inorg. Chem.* **1993**, *40*, 1.
(4) Romao, M. J.; Knablein, J.; Huber, R.; Moura, J. J. *Prog. Biophys. Mol. Biol.* **1997**, *68*, 121.
(5) Baker, S. C.; Kelly, D. P.; Murrel, J. C. *Nature* **1991**, *350*, 627. Charlson, R. J.; Lovelock, J. E.; Andreae, M. O.; Warren, S. G. *Nature* **1987**, *326*, 655.

10.1021/ic011169w CCC: $22.00
Published on Web 02/14/2002

(EXAFS) spectroscopy at the K-edge of the molybdenum center,[6,7] resonance Raman (rR) spectroscopy,[8−10] magnetic circular dichroism (MCD) spectroscopy,[11] and electron paramagnetic resonance (EPR) spectroscopy.[12] In addition, the enzymes isolated from both organisms have been studied by X-ray crystallography.[13−16] Enzymes isolated from these sources exhibit a high degree of sequence similarity (77% identity and 93.5% similarity) and are localized in the periplasmic space. Despite the similarities between these two enzymes, detailed descriptions of the active site have been the subject of intense debate.

The first crystallographic investigation on DMSO reductase isolated from *R. sphaeroides* was carried out in the oxidized form as well as on the dithionite reduced form.[13b] On the basis of the crystallographic results, a novel mechanism involving an oxygen-atom transfer reaction between a monooxo−Mo(VI) center and a desoxo−Mo(IV) center was proposed. Subsequently, crystal structures of the *R. capsulatus* protein described more conventional dioxo−Mo(VI) and monooxo−Mo(IV) centers.[14,17] Although there are major differences in the active-site descriptions, the structural reports reveal a close similarity with respect to the folding of the protein, the presence of two pyranopterin cofactors, and a single coordinated serine per molybdenum atom. Among the differences are the number of coordinated pyranopterin ene-1,2-dithiolate donors**,** the mode of their coordination (i.e., bidentate or monodentate), and the number of terminally coordinated oxo groups (O_t). Detailed EXAFS and rR data on the *R. sphaeroides* enzyme suggest a monooxo−Mo(VI) center coordinated by four sulfur donors.[7] A similar EXAFS investigation on the *R. capsulatus* enzyme suggested that the fully oxidized state had a dioxo−molybdenum center.[6] A high-resolution (1.3 Å) crystal structure of the *R. sphaeroides* enzyme that shows that the active site is disordered, existing as a mixture of hexa- and pentacoordinated molybdenum centers,[13a] has recently been reported. It has also been suggested that such structural disorders may be a result of different crystallization or protein-handling conditions. Indeed, by varying the preparative conditions, different forms of the *R. capsulatus* enzyme have been generated.[18] Another in-depth rR investigation on *R. capsulatus* raised the possibility of sulfeinic units resulting from the dithiolene moiety.[9] While these investigations have provided insight into the structure and biochemistry of DMSO reductase, it appears that the reduced and catalytically competent molybdenum center is desoxo−Mo(IV), while the fully oxidized state is a monooxo−Mo(VI) center. Similar reactivities with discrete inorganic complexes have recently been discovered.[19−21]

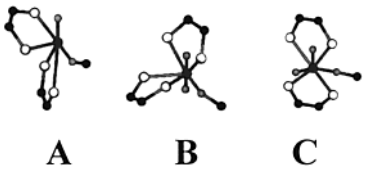

Figure 1. Active-site structures of (A) DMSO reductase from *R. sphaeroides*,[13] (B) TMAO reductase from *Shewanella massilia*,[23] and (C) DMSO reductase from *R. capsulatus*.[14] The O_t-Mo-O_{ser} angles are (A) 109°, (B) 146 and 90°, and (C) 77 and 93°.

We have been interested in understanding the chemical significance of the structural diversity of the active center, and recently we pointed out another geometric diversity (i.e., the geometric relationship between the terminal oxo (O_t) and serinato oxygen (O_{ser}) donors).[22] A detailed inspection of the DMSO reductase crystallographic data, and that of a related enzyme trimethylamine *N*-oxide reductase (TMAOR), reveals a wide variation in the reported O_t-Mo-O_{ser} angle, which ranges from 77−146° (Figure 1).[13−15,23] To understand the chemical significance of this angular variability, we reported the synthesis of two geometric isomers: *cis*-(L1O)$Mo^{V}OCl_2$ and *trans*-(L1O)$Mo^{V}OCl_2$ (where L1OH = (3-*tert*-butyl-2-hydroxy-5-methylphenyl)bis(3,5-dimethylpyrazolyl) methane) (Figure 2).[24] Here the cis and trans notations refer to the position of the phenolato oxygen (O_p) relative to that of the terminal oxo (O_t) ligand.

Using these well-defined**,** discrete molecules, we have suggested that by varying the O_t-Mo-O_p angle the elec-

(6) Baugh, P. E.; Garner, C. D.; Charnock, J. M.; Collison, D.; Davies, E. S.; McAlpine, A. S.; Bailey, S.; Lane, I.; Hanson, G. R.; McEwan, A. G. *J. Biol. Inorg. Chem.* **1997**, *2*, 634.
(7) George, G. N.; Hilton, J.; Temple, C.; Prince, R. C.; Rajagopalan, K. V. *J. Am. Chem. Soc.* **1999**, *121*, 1256. George, G. N.; Hilton, J.; Rajagopalan, K. V. *J. Am. Chem. Soc.* **1996**, *118*, 1113.
(8) (a) Garton, S. D.; Hilton, J.; Oku, H.; Crouse, B. R.; Rajagopalan, K. V.; Johnson, M. K. *J. Am. Chem. Soc.* **1997**, *119*, 12906. (b) Johnson, M. K.; Garton, S. D.; Oku, H. *J. Biol. Inorg. Chem.* **1997**, *2*, 797.
(9) Bell, A. F.; He, X.; Ridge, J. P.; Hanson, G. R.; McEwan, A. G.; Tonge, P. J. *Biochemistry* **2001**, *40*, 440.
(10) Gruber, S.; Kilpatrick, L.; Bastian, N. R.; Rajagopalan, K. V.; Spiro, T. G. *J. Am. Chem. Soc.* **1990**, *112*, 8179. Kilpatrick, L.; Rajagopalan, K. V.; Hilton, J.; Bastian, N. R.; Stiefel, E. I.; Pilato, R. S.; Spiro, T. G. *Biochemistry* **1995**, *34*, 3032.
(11) Benson, N.; Farrar, J. A.; McEwan, A. G.; Thomson, A. J. *FEBS Lett.* **1992**, *307*, 169−72. Finnegan, M. G.; Hilton, J.; Rajagopalan, K. V.; Johnson, M. K. *Inorg. Chem.* **1993**, *32*, 2616.
(12) Stewart, L. J.; Bailey, S.; Bennett, B.; Charnock, J. M.; Garner, C. D.; McAlpine, A. S. *J. Mol. Biol.* **2000**, *299*, 593. Bennett, B.; Benson, N.; McEwan, A. G.; Bray, R. C. *Eur. J. Biochem.* **1994**, *225*, 321.
(13) (a) Li, H.-K.; Temple, C.; Rajagopalan, K. V.; Schindelin, H. *J. Am. Chem. Soc.* **2000**, *122*, 7673. (b) Schindelin, H.; Kisker, C.; Hilton, J.; Rajagopalan, K. V.; Rees, D. C. *Science* **1996**, *272*, 1615.
(14) McAlpine, A. S.; McEwan, A. G.; Bailey, S. *J. Mol. Biol.* **1998**, *275*, 613. McAlpine, A. S.; McEwan, A. G.; Shaw, A. L.; Bailey, S. *J. Biol. Inorg. Chem.* **1997**, *2*, 690.
(15) Schneider, F.; Loewe, J.; Huber, R.; Schindelin, H.; Kisker, C.; Knaeblein, J. *J. Mol. Biol.* **1996**, *263*, 53. Knablein, J.; Dobbek, H.; Ehlert, S.; Schneider, F. *J. Biol. Chem.* **1997**, *378*, 293.
(16) Sato, K.; Sasaki, H.; Okubo, A.; Tanokura, M.; Yamazaki, S. *Proc. Jpn. Acad., Ser. B* **1997**, *73B*, 30.
(17) McEwan, A. G.; Hanson, G. R.; Bailey, S. *Biochem. Soc. Trans.* **1998**, *26*, 390.
(18) Bray, R. C.; Adams, B.; Smith, A. T.; Bennett, B.; Bailey, S. *Biochemistry* **2000**, *39*, 11258. Adams, B.; Smith, A. T.; Bailey, S.; McEwan, A. G.; Bray, R. C. *Biochemistry* **1999**, *38*, 8501.
(19) Arzoumanian, H.; Corao, C.; Krentzien, H.; Lopez, R.; Teruel, H. *J. Chem. Soc., Chem. Commun.* **1992**, 856.
(20) Sung, K.-M.; Holm, R. H. *J. Am. Chem. Soc.* **2001**, *123*, 1931. Lim, B. S.; Holm, R. H. *J. Am. Chem. Soc.* **2001**, *123*, 1920. Lim, B. S.; Sung, K.-M.; Holm, R. H. *J. Am. Chem. Soc.* **2000**, *122*, 7410. Lim, B. S.; Donahue, J. P.; Holm, R. H. *Inorg. Chem.* **2000**, *39*, 263. Donahue, J. P.; Goldsmith, C. R.; Nadiminti, U.; Holm, R. H. *J. Am. Chem. Soc.* **1998**, *120*, 12869. Donahue, J. P.; Lorber, C.; Nordlander, E.; Holm, R. H. *J. Am. Chem. Soc.* **1998**, *120*, 3259.
(21) Nemykin, V. N.; Davie, S. R.; Mondal, S.; Rubie, N.; Somogyi, A.; Kirk, M. L.; Basu, P. *J. Am. Chem. Soc.* **2002**, *124*, 756−757.
(22) Davie, S. R.; Rubie, N. D.; Hammes, B. S.; Carrano, C. J.; Kirk, M. L.; Basu, P. *Inorg. Chem.* **2001**, *40*, 2632.
(23) Czjzek, M.; Santos, J.-P. D.; Pommier, J.; Giordano, G.; Mejean, V.; Haser, R. *J. Mol. Biol.* **1998**, *284*, 435.
(24) Hammes, B. S.; Carrano, C. J. *Inorg. Chem.* **1999**, *38*, 3562.

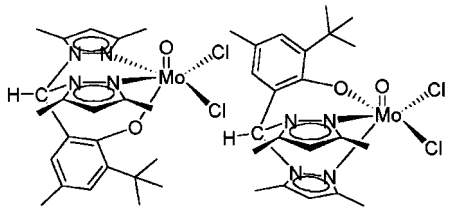

Figure 2. Schematic representation of the cis and trans isomers of the heteroscorpionate ligand, L1OH.

tronic structure and consequently the reduction potential could be modulated.[22] On the basis of these findings, we hypothesized that a "serine-gated electron-transfer" process may be important in the catalytic mechanism of DMSO reductase. Here we report an improved synthesis of the two isomers, the details of the isomeric transformation, the electronic structure of the two isomers, and the details of the serine-gated electron-transfer hypothesis and its mechanistic implication to DMSO reductase.

Experimental Section

All syntheses were carried out in oxygen-free, dry argon atmospheres using dry and distilled solvents following standard Schlenk techniques.

Materials and Supplies. All chemicals were purchased from commercial sources such as Aldrich Chemical Company and Acros Chemical Company. The solvents were purified as follows: acetonitrile from CaH_2 followed by $Na_2CO_3-KMnO_4$ and finally from P_2O_5; dichloromethane from CaH_2; toluene and tetrahydrofuran (THF) from sodium benzophenone. The ligand, L1OH, was synthesized as reported previously.[24]

Spectroscopy and Electrochemistry. Infrared spectra were recorded on a Perkin-Elmer FT-IR 1760X using KBr pellets. The electronic spectra were recorded on a Cary 14 spectrophotometer with an OLIS 14 version 2.6.99 operating system connected to a constant-temperature circulator. The kinetic measurements were performed at a series of seven temperatures ranging from 20 to 55 °C with a 5 °C increment in dry, oxygen-free acetonitrile. All kinetic data were transferred to a personal computer and processed using Origin 6.1 software from Microcal. Electrochemical measurements were carried out in a Bioanalytical Systems (BAS) model CV-50W. Voltammograms were recorded with a standard three-electrode system consisting of a Pt-disk working electrode, a Ag/Ag^+ reference electrode, and a Pt-wire auxiliary electrode. All voltammograms were internally referenced with ferrocene, and the potentials are reported with respect to the Fc^+/Fc couple without junction correction. Electrospray mass spectra (ESI MS) were collected on a Micromass ZMD mass spectrometer, with acetonitrile solutions injected via syringe pump at a flow rate of 0.1 mL/min.

Computational Details. The X-ray crystal geometries have been used for *cis*-(L1O)$MoOCl_2$ and *trans*-(L1O)$MoOCl_2$ complexes.[22] In the case of the twist mechanism, the trigonal face containing the O_t and two chlorine atoms was rotated about the pseudo-threefold axis in 10° increments. The single-point energies for each of the rotamers were calculated and plotted as a function of the angle of rotation. The rotational barrier was calculated as the energy difference between *cis*-(L1O)$MoOCl_2$ and the most unfavorable conformer, a 60° rotation of the trigonal face leading to an eclipsed conformation.[25,26] To understand the steric contribution to the twist mechanism of cis−trans isomerization, model calculations were carried out using a simplified structure obtained by deleting the extraneous alkyl groups. The rotational barrier in this set of calculations was determined in a manner similar to that described above. These calculations were performed at the semiempirical level with the PM3(tm) Hamiltonian[27] implemented in the Hyperchem software.[28] In addition, single-point calculations for *cis*-(L1O)-$MoOCl_2$, *trans*-(L1O)$MoOCl_2$, and *eclipsed*-(L1O)$MoOCl_2$ complexes were performed at the DFT level using Becke's three-parameter hybrid-exchange functional[29] and Perdew's nonlocal-correlation functional[30] (B3P86) in the borders of the unrestricted Hartree−Fock formalism. The B3P86 exchange-correlation functional was chosen because previous research has shown that this functional gives similar, and at times superior, results compared to those from the Becke three-parameter hybrid-exchange functional[29] and the Lee−Yang−Parr nonlocal-correlation functional (B3LYP)[31] when energies profiles are calculated.[32,33] For all DFT calculations, the molybdenum atom is represented by DGauss full-electron double-ζ basis sets with polarization having a (18s,12p,9d) → [6s,-5p,3d] contraction scheme,[34] while a standard 6-311G* basis set[35] was used to describe all other atoms. All DFT calculations were performed using the Gaussian 98 family of software for Windows and Linux operating systems.[36]

Kinetic Analysis. The kinetic measurements were carried out in dry, degassed acetonitrile solutions prepared under an argon atmosphere using standard Schlenk techniques. Measurements were performed in 1 cm path-length quartz cuvettes placed in an isothermal cell holder. In each case, the first data point was collected within one minute of dissolution of the solid sample. Assays were conducted by monitoring the changes in the absorption at 347 nm.

(25) Nemykin, V. N.; Kobayashi, N.; Chernii, V. Y.; Belsky, V. K. *Eur. J. Inorg. Chem.* **2001**, 733.
(26) Grodzicki, M.; Flint, H.; Winkler, H.; Walker, F. A.; Trautwein, A. X. *J. Phys. Chem. A* **1997**, *101*, 4202.
(27) Stewart, J. I. P. *J. Comput.-Aided Mol. Des.* **1990**, *4*, 1.
(28) *HyperChem Pro*, version 6.03; HyperCube, Inc.: Gainesville, FL, 2001.
(29) Becke, A. D. *J. Chem. Phys.* **1993**, *98*, 5648.
(30) Perdew, J. P. *Phys. Rev. B: Condens. Matter* **1986**, *33*, 8822.
(31) Lee, C.; Yang, W.; Parr, R. G. *Phys. Rev. B: Condens. Matter* **1988**, *37*, 785.
(32) Thomson, L. M.; Hall, M. B. *J. Am. Chem. Soc.* **2001**, *123*, 3995.
(33) Neumann, R.; Nobes, R. H.; Handy, N. C. *Mol. Phys.* **1996**, *87*, 1. Wilberg, K. B.; Stratmann, R. E.; Frisch, M. J. *Chem. Phys. Lett.* **1998**, *297*, 60.
(34) Basis sets were obtained from the Extensible Computational Chemistry Environment Basis Set Database, version 4/22/01, as developed and distributed by the Molecular Science Computing Facility, Environmental and Molecular Sciences Laboratory, which is part of the Pacific Northwest Laboratory, P.O. Box 999, Richland, WA 99352, and funded by the U.S. Department of Energy. The Pacific Northwest Laboratory is a multiprogram laboratory operated by Battelle Memorial Institute for the U.S. Department of Energy under contract DE-AC06-76RLO 1830. Contact David Feller or Karen Schuchardt for further information.
(35) McLean, A. D.; Chandler, G. S. *J. Chem. Phys.* **1980**, *72*, 5639. Krishnan, R.; Binkley, J. S.; Seeger, R.; Pople, J. A. *J. Chem. Phys.* **1980**, *72*, 650.
(36) Frisch, M. J.; Trucks, G. W.; Schlegel, H. B.; Scuseria, G. E.; Robb, M. A.; Cheeseman, J. R.; Zakrzewski, V. G.; Montgomery, J. A., Jr.; Stratmann, R. E.; Burant, J. C.; Dapprich, S.; Millam, J. M.; Daniels, A. D.; Kudin, K. N.; Strain, M. C.; Farkas, O.; Tomasi, J.; Barone, V.; Cossi, M.; Cammi, R.; Mennucci, B.; Pomelli, C.; Adamo, C.; Clifford, S.; Ochterski, J.; Petersson, G. A.; Ayala, P. Y.; Cui, Q.; Morokuma, K.; Malick, D. K.; Rabuck, A. D.; Raghavachari, K.; Foresman, J. B.; Cioslowski, J.; Ortiz, J. V.; Stefanov, B. B.; Liu, G.; Liashenko, A.; Piskorz, P.; Komaromi, I.; Gomperts, R.; Martin, R. L.; Fox, D. J.; Keith, T.; Al-Laham, M. A.; Peng, C. Y.; Nanayakkara, A.; Gonzalez, C.; Challacombe, M.; Gill, P. M. W.; Johnson, B. G.; Chen, W.; Wong, M. W.; Andres, J. L.; Head-Gordon, M.; Replogle, E. S.; Pople, J. A. *Gaussian 98*; Gaussian, Inc.: Pittsburgh, PA, 1998.

The rate constants were determined from eq 1,

$$\frac{d[cis\text{-(L1O)MoOCl}_2]}{dt} = A_0 + [cis\text{-(L1O)MoOCl}_2]\exp(-t/\tau) \quad (1)$$

where A_0 is the initial absorbance, t is the time in minutes, and τ is the half-life of the reaction. In all cases, the data were fit to the above single-exponential with $R^2 = 0.99$ or better, with the residual absorbances an order of magnitude lower than the measured ones. From the variable-temperature experiments, the activation parameters were calculated using the Arrhenius and Eyring equations (eqs 2a and b),

$$\ln k = \ln A - \frac{E_a}{RT} \quad (2a)$$

$$-\ln \frac{kh}{k_B T} = \frac{\Delta H^{\ddagger}}{RT} - \frac{\Delta S^{\ddagger}}{R} \quad (2b)$$

where all parameters are of the usual significance.

Synthesis of *cis*-(L1O)MoOCl$_2$. $MoCl_5$ (280 mg, 1.03 mmol) was placed in a dry 25 mL Schlenk flask, and 10 mL of dry degassed THF was added at −78 °C using an acetone−dry ice bath with stirring for 1 h. The temperature of the resulting slurry was raised to ∼0 °C by placing the reaction flask in an ice bath. To this greenish-brown solution was added 375 mg (1.02 mmol) of the L1OH under the argon atmosphere, and the reaction mixture was stirred overnight on ice. The color of the solution changed to dark brown. The solution was filtered and washed with acetonitrile, and the residue was extracted with dichloromethane. The resulting solution was combined with the filtrate, evaporated to dryness, redissolved in dichloromethane, and chromatographed on silica gel using chloroform as the eluent. The target compound eluted from the column as the second pink band. Yield: 200 mg (37%).

Synthesis of *trans*-(L1O)MoOCl$_2$. From the column described above, a yellow band was eluted as the fourth band. Yield: 100 mg (18%). The first yellow band (minor) was due to the (L1O)-MoO_2Cl, while the third brown band was determined to be a mixture of the cis and trans isomers, accounting for ∼100 mg of the product. Thus, the total yield of the two isomers was 400 mg (74%).

Results

The oxo−Mo(V) dichloride complex of the hydrotris(pyrazolyl)borate ligand has been synthesized using $MoCl_5$ as the source of molybdenum. In our initial communication, we have reported the synthesis of the pure *cis*-(L1O)Mo^V-OCl_2 following a similar procedure.[22] However, the kinetic investigation demonstrates that the cis isomer spontaneously converts to the more-stable trans isomer (vide infra), suggesting that a higher yield of the *cis*-(L1O)Mo^VOCl_2 could be obtained by conducting the synthesis at low temperatures. Using this modification, we have synthesized the *cis*-(L1O)-Mo^VOCl_2 as the kinetically controlled product in a higher yield. Statistically, the cis isomer should be the major (67%) product, and the trans isomer should be the minor (33%) product. The experimentally obtained yield follows this statistical distribution (37% cis and 18% trans), indicating that very little of the cis isomer had isomerized to the trans isomer. The cis complex is highly soluble in common chlorinated organic solvents such as chloroform and dichloromethane, while the yellow trans compound shows lower solubility under the same conditions. The molecular composition of the two compounds was confirmed by electrospray ionization mass spectrometry (ESI MS) of acetonitrile solutions of the complexes. Slow evaporation of a dichloromethane or an acetonitrile solution of the cis compound afforded X-ray-quality single crystals; however, disorder in the crystal did not allow us to determine the geometry unequivocally.[22]

Both isomers exhibit well-defined Mo═O vibrations in the IR spectra. The Mo═O stretching frequency of the cis isomer appears at 961 cm^{-1}, while the same vibration appears at 947 cm^{-1} for the trans isomer. The cis complex has a low-energy charge-transfer band that originates from the phenolic oxygen-to-molybdenum transition (vide infra). This charge-transfer band precludes the observation of the ligand-field transition. No such low-energy charge-transfer band could be observed for the trans isomer, which would allow the observation of the ligand-field transition.[37]

The redox chemistry of the two isomers was investigated by cyclic voltammetry in acetonitrile solution, which is depicted in Figure 3. Both compounds exhibit well-defined one-electron reductive couples that can be attributed to the reduction of Mo(V) to Mo(IV), with the half-wave potentials of −934 and −1150 mV (vs Fc^+/Fc) for the trans and the cis isomers, respectively. The peak-to-peak separations (83 and 62 mV, respectively, for the cis and trans isomers) are indicative of the quasi-reversible one-electron nature of the process. In addition, both isomers exhibit well-defined one-electron oxidative couples for the oxidation of Mo(V) to Mo(VI). The cis isomer is easier to oxidize ($E_{1/2}$ = 726 mV vs Fc^+/Fc; ΔEp = 70 mV) than the trans isomer ($E_{1/2}$ = 861 mV vs Fc^+/Fc; ΔEp = 65 mV). For both couples, the peak currents follow linear relationships with the square root of the scan rate. Interestingly, the separation between the two couples is larger in the cis isomer (1876 mV) than in the trans isomer (1795 mV). Although a similar reductive couple at −250 mV (vs Ag/AgCl) has been observed for Tp*$MoOCl_2$ (where Tp* is the hydrotris(3,5-dimethylpyrazolyl)borate ligand), no oxidative couple was detected for this complex.[38]

The cis isomer spontaneously isomerizes to the trans isomer, which is associated with distinctive changes in the optical spectra. The difference spectra of the isomer transformation are provided in Figure 4 and exhibit tight isosbestic points at 466 and 316 nm. The rates of the isomeric conversions have been followed spectrophotometrically at 347 nm. In each case, the reaction was monitored for 3−5 half-lives to ensure that the process had neared completion. In an attempt to provide the best possible approximation to the theromodynamic parameters associated with the conversion, the reaction rate was measured over seven different temperatures ranging from 25 to 55 °C. The isomerization follows a first-order process, indicating a unimolecular reaction. All data are tabulated in Table S-I (Supporting Information), with a representative fit shown in Figure 5.

(37) Rubie, N.; Davie, S. R.; Kail, B.; Hammes, B. S.; Carrano, C. J.; Basu, P.; Kirk, M. L. Manuscript in preparation.
(38) Cleland, W. E., Jr.; Barnhart, K. M.; Yamanouchi, K.; Collison, D.; Mabbs, F. E.; Ortega, R. B.; Enemark, J. H. *Inorg. Chem.* **1987**, *26*, 1017.

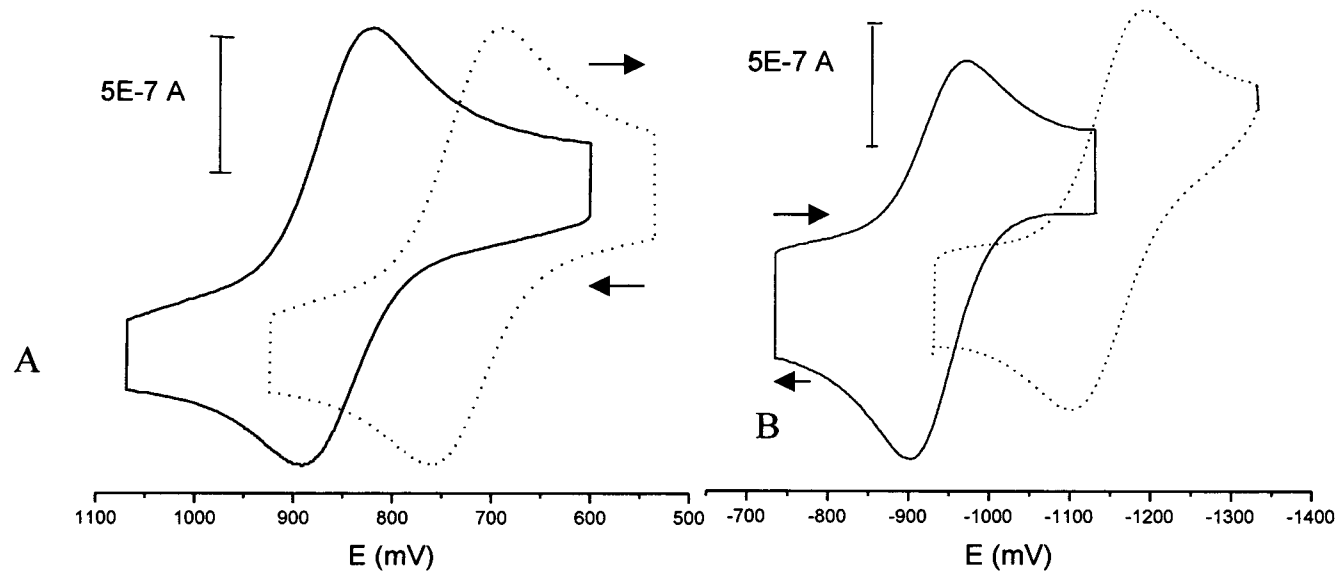

Figure 3. Cyclic voltammograms of the two isomers: cis (dashed line) and trans (solid line). For both isomers, panel A represents the oxidative couple and panel B represents the reductive couple. The voltammograms were recorded with a standard three-electrode configuration in acetonitrile at 22 °C (see text). Potentials are presented with respect to the Fc^+/Fc couple.

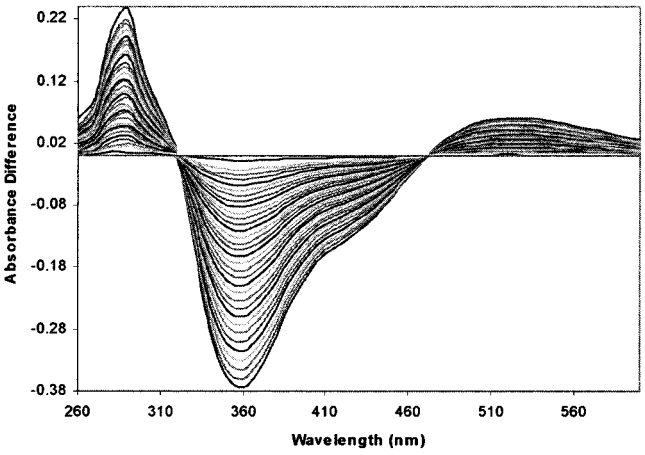

Figure 4. Optical difference (absorbance at time *t* minus the final absorbance) spectra showing clear isosbestic points for the isomeric conversion. Spectra were recorded at 22 °C in acetonitrile.

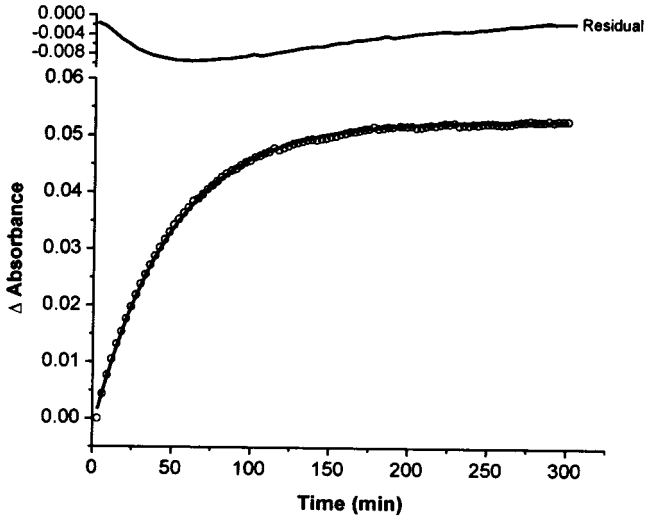

Figure 5. Change in the absorbance difference at 347 nm as a function of time. The assay was conducted in acetonitrile at 55 °C. The exponential fit and the residuals are also shown.

These first-order rate constants, obtained from the fits, were used to determine the activation parameters. Thus, the activation energy and the frequency factor were determined from the Arrhenius equation (eq 2) to be $E_a = 21.7 \pm 0.4$ kcal/mol and $\ln A = 26.2 \pm 0.6$. Similarly, the enthalpy (20 ± 3 kcal/mol) and the entropy (−9 ± 1 cal/mol K) of activation were determined from the Eyring relation (eq 2). All thermodynamic and activation parameters can be summarized by the free-energy relationship depicted in Figure 6, which indicates the cis isomer to be approximately 5 kcal/mol less stable than the trans isomer.

The kinetic results were complemented by ESI MS on (L1O)MoO_2Cl, with and without the addition of excess tetraalkylammonium salts (R_4NX, where R = ^{n}Bu, X = F or I or where R = ^{n}Et, X = Br). The results of the ESI MS with and without tetraalkylammonium salts present are displayed in Chart 1. All Mo(V) species discussed below gave good-quality ESI MS, which were observed only in the negative-ion mode.

These experiments were performed by incubating 2.3 μmol of the *cis*-(L1O)MoO_2Cl in acetonitrile containing 4.8 μmol of R_4NX at 24 °C for 4 h with 2.4 μmol of the *trans*-(L1O)-MoO_2Cl incubated under the same conditions as those used in a control experiment. An additional control was introduced through incubation of equimolar concentrations of the cis and trans isomers in acetonitrile at 24 °C for 4 h. The experiments without R_4NX demonstrate that both isomers exhibit, in addition to their molecular-ion peaks, peak clusters due to the formation of (L1O)MoO_2Cl. With the exception of the fluoride salt, the experiments with R_4NX exhibit four additional peak clusters whose mass-to-charge ratios were well-matched to those expected for $[(L1O)Mo^{VI}O_2Cl]X^-$, $[(L1O)Mo^{VI}O_2Cl]Cl^-$, $[(L1O)Mo^{V}OCl_2]X^-$, and $[(L1O)$-$Mo^{V}OCl_2]Cl^-$. Additional identification of each peak cluster was made through the simulation of the experimentally observed isotopic distribution pattern. Under similar experi-

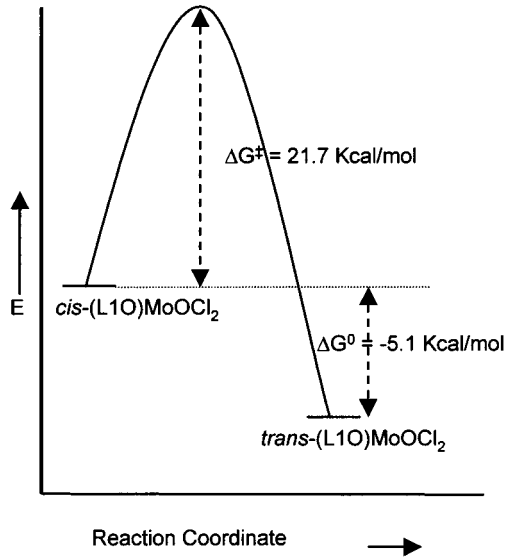

Figure 6. Experimentally determined free-energy relations of the two isomers. Note that the difference in thermodynamic stabilities is obtained from the reductive couples.

Chart 1. ESIMS of (L1O)$MoOCl_2$ with Base Peaks in Parentheses

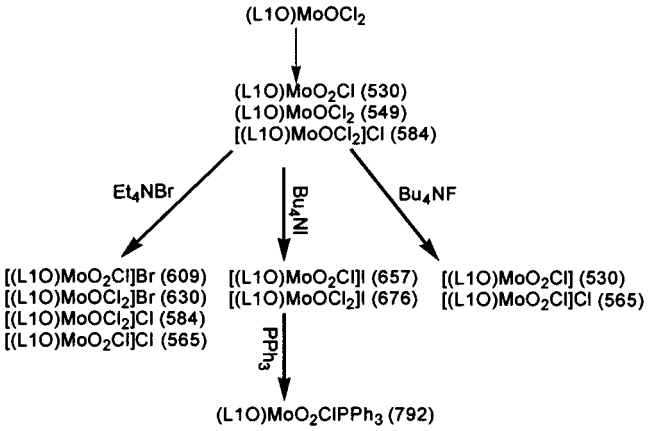

mental conditions (e.g., concentration, spectrometer parameters, flow rate, etc.), the intensity of the signal due to the oxidized Mo(VI) species was higher for the cis complex than that for the trans isomer. In the case of the dioxo species, the comparison with the mass spectra of an authentic dioxo complex confirmed its presence in the cis and trans spectra. The basis for the latter experiments is that tertiary phosphines are well-known, selective, oxo-abstracting agents in which a terminal oxo group may be abstracted from a dioxo species but not from a monooxo species. We have recently shown that mass spectrometry is a powerful tool for studying the oxygen-atom transfer reaction by probing the intermediates of the process.[39] In accord with this result, when the authentic dioxo complex and the cis and trans isomers were reacted with excess PPh_3, a peak cluster due to a phosphine adduct could be detected in all cases, further confirming the presence of a dioxo species in solution.

The effects of the observed geometries on the electronic structure were investigated computationally. The electronic

(39) Smith, P. D.; Millar, A. J.; Young, C. G.; Ghosh, A.; Basu, P. *J. Am. Chem. Soc.* **2000**, *122*, 9298.

Table 1. Composition of Orbitals Containing Mo d Manifolds[a]

orbital	geometry	*E*, eV	% Mo	% O	% Cl	% OPh	% Pz	% L1O
d_{xy}	trans	−6.63446	64.62	0.01	29.51	0.76	4.63	5.39
	cis	−6.05921	51.48	0.94	11.42	34.19	1.55	35.78
	eclipsed	−5.92587	58.03	3.14	14.25	13.88	8.47	23.29
d_{xz}	trans	−3.04525	69.42	14.23	2.58	9.55	3.54	13.09
	cis	−3.54703	66.94	15.70	4.03	1.69	10.19	12.12
	eclipsed	−3.16308	60.43	8.19	15.84	2.43	11.95	14.64
d_{yz}	trans	−2.9247	66.54	14.48	1.96	11.85	4.19	16.04
	cis	−3.36635	68.80	13.26	4.61	3.51	8.47	12.44
	eclipsed	−2.92552	68.74	10.76	6.94	6.01	6.34	12.89
$d_{x^2-y^2}$	trans	−1.6629	34.07	0.01	11.30	14.05	38.31	52.35
	cis	−1.21092	50.84	0.25	16.50	8.92	18.00	30.27
	eclipsed	−1.34507	39.02	2.40	7.36	14.42	29.70	48.95
d_{z^2}	trans	0.66614	22.82	1.85	3.03	52.72	13.40	66.13
	cis	0.46613	28.35	4.35	2.87	7.82	33.20	44.24
	eclipsed	−0.00463	22.81	4.05	3.68	13.99	46.80	64.12

[a] Only the orbitals with α-spin are shown.

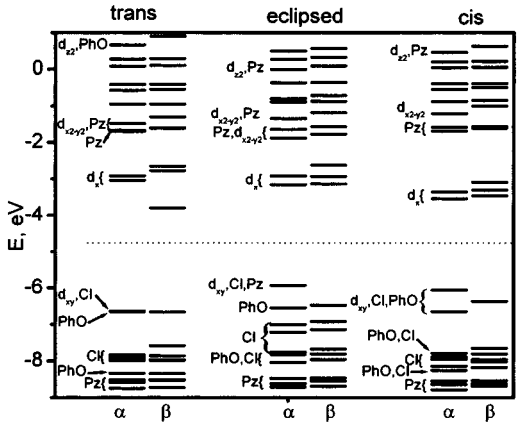

Figure 7. Molecular orbital diagrams of the cis, trans and eclipsed geometries. Spin-unrestricted calculations were carried out using the B3P86 DFT method. Basis set descriptions are in the text.

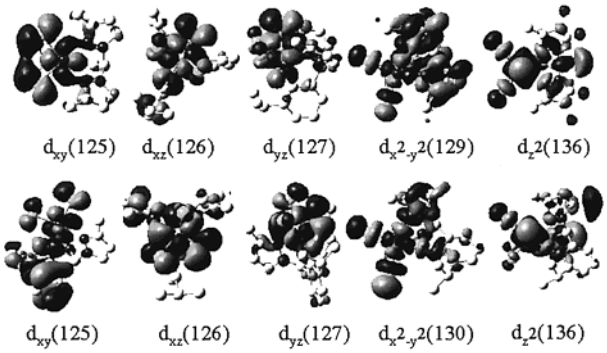

Figure 8. Selected molecular orbitals (α-spin) in the cis and trans isomers containing the metal d manifold. The orbital numbers are shown in the parentheses. The d_{xy} orbital (125) is occupied, while the others orbitals are virtual. Top panel, trans isomer; bottom panel, cis isomer.

structure calculations for *cis*-, *trans*-, and *eclipsed*-(L1O)-$MoOCl_2$ geometries were carried out at the unrestricted DFT B3P86 level. For computational purposes, the three-methyl groups (those distal to the metal center) were omitted from the model (Figure 2) as they do not significantly affect the steric requirement at the metal center. The energy-level diagram and orbital compositions are presented in Table 1 and Figures 7 and 8.

The calculations show that the metal d orbitals are strongly destabilized by strong antibonding interactions with the terminal oxo group as well as with the donor atom trans to

the terminal oxo group (i.e., phenolic oxygen for the trans isomer and pyrazolyl nitrogen for cis isomer). These interactions raise the energy of an orbital that is primarily composed of the metal d_{z^2} orbital that is higher than any of the other d orbitals. In all compounds, large contributions from the equatorial ligands to the $d_{x^2-y^2}$ orbital that lead to strong L^{σ}−Mo antibonding interactions have been observed. In each case, the displacement of the molybdenum atom from the equatorial plane (containing two chlorine, one nitrogen, and one oxygen or nitrogen atom) leads to an effective movement of the $d_{x^2-y^2}$ orbital away from the Mo−Cl, Mo−N, or Mo−O bond vectors. Such movement of the metal away from the equatorial plane reduces the L^{σ}−Mo overlap and stabilizes the $d_{x^2-y^2}$ orbital more than it does the d_{z^2} orbital. The molecular orbital containing the metal $d_{x^2-y^2}$ orbital contains several pyrazole π orbitals (Figure 7). Thus, the contribution to this orbital from the pyrazole π orbitals is greater in the trans isomer than in the cis. In addition to the previously discussed orbital interaction, the terminal oxo group contributes to a predominantly metal-centered lowest unoccupied molecular orbital (LUMO) and to LUMO + 1 orbitals through strong O^{π}−Mo(d_{xz}, d_{yz}) antibonding interactions. As expected, the lowest-energy d orbital is the d_{xy} orbital, which is the highest occupied molecular orbital (HOMO) and is half-filled for the molybdenum(V) state. In all cases, one orbital that is predominantly due to the phenolic group could be located below the metal manifold. This orbital and the HOMO are well-separated from the other occupied π orbitals that are predominantly localized on the chlorine and the L1O$^-$ pyrazole or phenolic groups (Figure 7). The differences in energy between HOMO and HOMO − 1 are 0.02 and ∼0.6 eV for the trans and cis (also the eclipsed) geometries, respectively.

Discussion

Electronic Structures of the (L1O)MoOCl$_2$ Complexes. In general, electronic structure calculations of transition-metal complexes are carried out with simplified ligand architectures.[32,40−44] Although simplified ligand architectures are computationally less expensive, they were not able to profile our system accurately. In fact, when these approximations were applied to the cis and trans isomers, the cis isomer was found to be more stable than the trans. Therefore, we conducted all electronic structure calculations with near-complete ligand architecture, with only the distal methyl groups excluded. In addition, a large basis set for the molybdenum atom was employed for all calculations. Although this strategy increased the computational requirements, it revealed a number of differences in the electronic structures compared to those obtained by calculations conducted on simplified ligand architectures.[45]

As expected, the molybdenum metal d-fold splitting follows the order $d_{xy} < d_{xz}$ and d_{yz} (nearly degenerate) < $d_{x^2-y^2} < d_{z^2}$, with d_{z^2} being the most destabilized orbital. The contribution of the L1O$^-$ ligand to the destabilization of the d_{z^2} orbital is revealed from the Walsh-like diagram for the cis, eclipsed , and trans geometries (Figure 7). A higher destabilization of the d_{z^2} orbital is observed for the trans isomer and is due to the negative charge of the phenolic oxygen atom.

As discussed earlier, the deviation of the molybdenum atom from the *xy* plane reduces the L^{σ}−Mo overlap and thus stabilizes this orbital with respect to the d_{z^2} orbital. The composition of the $d_{x^2-y^2}$ orbital is clearly indicative of significant mixing between the metal-based orbitals and the orbitals from the atoms of the L1O$^-$ ligand. A similar situation has recently been reported for a series of molybdenum complexes with tetrathiophenolates.[40a,42] In agreement with the strength of pyrazole π orbitals,[46] several low-lying pyrazole orbitals could be located within the metal manifolds by DFT calculations (Figure 7). Similar situations have been described previously.[47] This observation suggests that, for electronic structure calculations, it is important to use geometries that closely resemble the actual architecture instead of simplified or truncated versions. DFT calculations on simplified models with identical basis sets, where pyrazole and phenolate rings are represented by ammonia and methoxide groups, respectively, show poor agreement with the experimental data. As mentioned earlier, these calculations show the cis isomer to be more stable than the trans.[45]

Bonding of the terminal oxygen to molybdenum has been intensely investigated.[40b,42,48] The molybdenum-to-oxygen terminal bonds consist of a σ interaction (between the O p_z orbital and the Mo d_{z^2} orbital) and two π interactions (between the O p_x and p_y orbitals and the Mo d_{π} orbitals). A similar orbital picture can be used to describe the bonding between the molybdenum atom and the axial (axial to the terminal oxo group) donor atom. Stronger π and σ interactions with the axial donor strongly destabilize the d_{z^2} and the d_{π} orbitals of molybdenum. In the trans isomer, the axial oxygen from the L1O$^-$ ligand, being a stronger σ and π donor than nitrogen in the cis isomer, destabilizes both the d_{z^2} and the d_{π} orbitals by 0.2 and 0.5 eV, respectively (Figure

(40) (a) McMaster, J.; Carducci, M. D.; Yang, Y.-S.; Solomon, E. I.; Enemark, J. H. *Inorg. Chem.* **2001**, *40*, 687. (b) Izumi, Y.; Glaser, T.; Rose, K.; McMaster, J.; Basu, P.; Enemark, J. H.; Hedman, B.; Hodson, K. O.; Solomon, E. I. *J. Am. Chem. Soc.* **1999**, *121*, 10035.
(41) (a) Webster, C. E.; Hall, M. B. *J. Am. Chem. Soc.* **2001**, *123*, 5820. (b) Pietsch, M. A.; Hall, M. B. *Inorg. Chem.* **1996**, *35*, 1273.
(42) McNaughton, R.; Tipton, A. A.; Rubie, N. D.; Conry, R.; Kirk, M. L. *Inorg. Chem.* **2000**, *39*, 5697.
(43) Bray, M. R.; Deeth, R. J. *Inorg. Chem.* **1996**, *35*, 5720.
(44) Ilich, P.; Hille, R. *J. Phys. Chem. B* **1999**, *103*, 5406. Voityuk, A. A.; Albert, K.; Romão, M. J.; Huber, R.; Rösch, N. *Inorg. Chem.* **1998**, *37*, 176.
(45) Nemykin, V. N.; Basu, P. Manuscript in preparation.
(46) Nemykin, V. N.; Polshina, A. E.; Polshin, E. V.; Kobayashi, N. *Mendeleev Commun.* **2000**, 54. Nemykin, V. N.; Polshina, A. E.; Chernii, V. Y.; Polshin, E. V.; Kobayashi, N. *J. Chem. Soc., Dalton Trans.* **2000**, 1019.
(47) Detrich, J. L.; Konecný, R.; Vetter, W. M.; Doren, D.; Reingold, A. L.; Theopold, K. H. *J. Am. Chem. Soc.* **1996**, *118*, 1703. Gunnoe, T. B.; Meiere, S. H.; Sabat, M.; Harman, W. D. *Inorg. Chem.* **2000**, *39*, 6127. Zaric, S.; Hall, M. B. *J. Phys. Chem. A* **1998**, *102*, 1963.
(48) Miskowski, V. M.; Gray, H. B.; Hopkins, M. D. *Adv. Transition Met. Coord. Chem.* **1996**, *1*, 159. Mayer, J. M. *Comments Inorg. Chem.* **1988**, *8*, 125. Solomon, E. I. *Comments Inorg. Chem.* **1984**, *3*, 227. Carducci, M. D.; Brown, C.; Solomon, E. I.; Enemark, J. H. *J. Am. Chem. Soc.* **1994**, *116*, 11856. Sabel, D. M.; Gewirth, A. A. *Inorg. Chem.* **1994**, *33*, 148. Neuhaus, A.; Veldkamp, A.; Frenking, G. *Inorg. Chem.* **1994**, *33*, 5278. Deeth, R. J. *J. Chem. Soc., Dalton Trans.* **1991**, 1895.

7). As a result, the Mo═O bond is weakened in the trans isomer. This situation is manifested in the Mo═O stretching frequencies in the two isomers: in the cis isomer, the Mo═O bond vibrates 14 cm^{-1} higher in energy than does the trans isomer. In the eclipsed geometry, on the other hand, the d_{z^2} orbital is destabilized only by the terminal oxo ligand; this destabilization enhances the energy difference between the $d_{x^2-y^2}$ and d_{z^2} orbitals to more than 1 eV (Figure 7).

It is instructive to point out that the redox orbital in oxo−Mo(V) complexes is primarily composed of the molybdenum d_{xy} orbital, with large contributions from the equatorial donor atoms.[40a,49,50] The antibonding interaction with equatorial chlorine atoms contributes nearly 30% to the HOMO of the trans compound; however, this contribution is smaller in the cis and the eclipsed geometries (∼11% for cis and ∼14% for eclipsed isomers, respectively). For both the cis and eclipsed geometries, the contribution from the $L1O^-$ ligand is increased. In the cis isomer, the antibonding interaction due to the phenolic group of the $L1O^-$ ligand is ∼36%. Such effective mixing between the d_{xy} and ligand π orbitals has been noted for the oxo−Mo(V) complexes coordinated by thiolate donors.[40a,42] The net result of this interaction is the overall destabilization of the half-filled HOMO in the cis isomer by ∼0.6 eV relative to the trans isomer. This destabilization is consistent with the observed position of the reductive and oxidative couples for the cis isomer. Indeed, experimentally, a difference of ∼100 mV was observed between oxidative couples of the cis and trans isomers, while a difference of 216 mV was observed for the reductive couples. In contrast to the equatorial-donor-atom contribution to the HOMO, the contribution from the axial donor (axial to the terminal oxo group) contributes negligibly to this orbital. Thus, from an electronic point of view, the six-coordinate complexes with heteroscorpionate ligands behave like square-pyramidal pentacoordinate complexes (e.g., tetrathiolate complexes of molybdenum, where the metal center is coordinated by four equatorial thiolato sulfur atoms). The same description also holds for the more popular hydrotris(3,5-dimethylpyrazolyl)borate ligand (Tp*).[45]

Therefore, it is evident that, both experimentally and computationally, the trans isomer is more stable than the cis isomer. The increased stability of the trans isomer may be accounted for by two distinct arguments involving electronic and steric components. First, the electronic structural calculations demonstrate that the half-filled molecular orbitals of the cis and trans isomers differ significantly in both their compositions and energetic properties. The cis isomer possesses a relatively strong antibonding interaction between the molybdenum d_{xy} orbital and the π orbitals of the phenolato oxygen atom; however, such an interaction is not present in the trans isomer. This interaction raises the energy of the HOMO in the cis isomer.

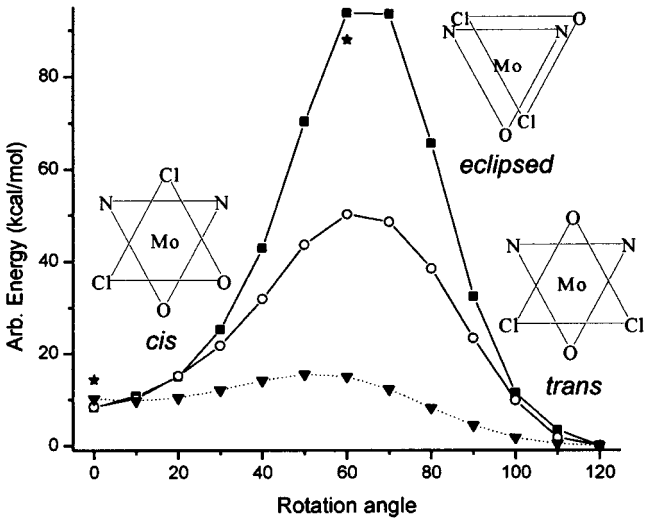

Figure 9. Calculated energy profile for the twist mechanism. The top trace represents the calculation with no optimization of the methyl group position. The middle trace represents the energy profile when the methyl groups are placed at energetically favorable positions. The bottom trace represents the energy profile without the ^{t}Bu and methyl groups. The asterisks represent energy calculated by the B3P86 DFT method, while all other calculations were done at the semiempirical (PM3(tm)) level. For details, see text.

In addition to the electronic factor discussed above, there is a steric component that accounts for the higher stability of the trans isomer. In the trans isomer, a strong trans influence of the terminal oxo group elongates the molybdenum−phenolic oxygen bond. As a consequence of this elongation, the bulky ^{t}Bu group is positioned farther from the methyl groups of the pyrazol rings. This stereochemical arrangement in the trans isomer makes the molybdenum center less crowded and thus more stable.

In an attempt to fully clarify the importance of this steric factor, the stability of the cis and trans isomers was calculated at the semiempirical (PM3(tm)) level with and without the bulky alkyl groups (Figure 9). By computation, it was determined that steric considerations were accountable for only about 20% of the relative stability of the trans isomer over the cis isomer and as such indicate that electronic factors play the dominant role in controlling the stability. Ongoing investigations in our laboratory should enhance the understanding of the origins behind this observed stability difference.

Mechanism of the Isomerization. In general, the mechanisms of geometric isomerization in coordination complexes have been studied in detail;[51] however, such studies on oxo−molybdenum complexes are very rare.[52] Even more rare is geometric isomerization in oxo−molybdenum complexes where three sites are occupied by a facially coordinating

(49) Helton, M. E.; Kirk, M. L. *Inorg. Chem.* **1999**, *38*, 4384. Inscore, F. E.; McNaughton, R.; Westcott, B. L.; Helton, M. E.; Jones, R.; Dhawan, I. K.; Enemark, J. H.; Kirk, M. L. *Inorg. Chem.* **1999**, *38*, 1401.

(50) Mondal, S.; Basu, P. *Inorg. Chem.* **2001**, *40*, 192. Nemykin, V. N.; Mondal, S.; Basu, P. Manuscript in preparation.

(51) Serpone, N.; Bickley, D. G. *Prog. Inorg. Chem.* **1972**, *17*, 391.

(52) (a) For isomerism in non-oxo−molybdenum complexes, see Argyropoulos, D.; Mitsopoulou, C.-A.; Katakis, D. *Inorg. Chem.* **1996**, *35*, 5549. (b) For isomerism in monooxo−molybdenum complexes, see Mondal, J. U.; Zamora, J. G.; Kinon, M. D.; Schultz, F. A. *Inorg. Chim. Acta* **2000**, *309*, 147. Barnard, K. R.; Bruck, M.; Huber, S.; Grittini, C.; Enemark, J. H.; Gable, R. W.; Wedd, A. G. *Inorg. Chem.* **1997**, *36*, 637. (c) For isomerism in dioxo−molybdenum complexes, see Duhme, A.-K. *J. Chem. Soc., Dalton Trans.* **1997**, 773.

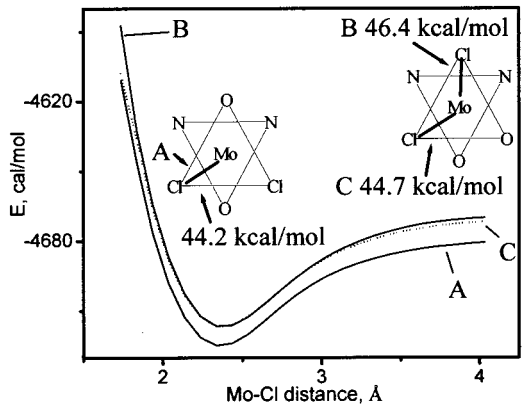

Figure 10. Calculated energies for the Mo−Cl bond dissociation for the two isomers. Calculations were carried out at the semiempirical (PM3-(tm)) level. Trace A represents the energy of dissociation of the Mo−Cl bond in the trans isomer. Traces B and C represent the energies of dissociation of the Mo−Cl bond; in B, the Mo−Cl bond trans to the phenolic oxygen is represented, and C represents the Mo−Cl bond cis to the phenolic oxygen.

ligand, and to our knowledge the mechanisms of such isomerization reactions have not been reported in detail. In general, there are two major processes by which isomerization reactions may proceed: the twist mechanism and the dissociative mechanism. In the case of the twist mechanism, the geometric rearrangement originates through a rotation about a pseudo-three-fold axis at the middle of a trigonal face (Figure 9). In contrast, the dissociative mechanism proceeds via geometric rearrangements through breaking of metal−ligand bonds, followed by reconstitution at a stereochemically different position relative to the first (Figure 10). With these possible mechanisms, two distinct types of dissociative interactions may be immediately ruled as unlikely possibilities. First, it is unlikely that a metal−ligand bond from the tridentate ligand will be broken because of a high entropic penalty. Second, it is improbable that the terminal oxo bond (a metal−ligand multiple bond) will dissociate in dry organic solvents. Thus, the only probable dissociative pathway, if this mechanism is operable, must involve the dissociation of a metal−halide bond. In addition, variable-temperature kinetic measurements demonstrate a negative entropy of activation, which is suggestive of a more-ordered transition state relative to that of the cis isomer. The negative entropy provides evidence that the bond dissociation pathway may not be a likely mechanism. Unfortunately, the magnitude of the entropy of activation is too small to definitely assign as a twist mechanism.

To understand the relative ease of the two mechanistic possibilities, the energy associated with the two processes has been computed at the PM3(tm) level. The energy profiles of the two processes are shown in Figures 9 and 10. For the twist mechanism, the OCl_2 face, consisting of the axial terminal-oxo group and the two equatorial chlorine atoms of the octahedron, was rotated from 0 to 120° with a 10° interval along the pseudo-three-fold axis. As expected, the 60° rotation provides an eclipsed conformation with the highest energy: 85.37 kcal/mol (73.65 kcal/mol from DFT calculations). To determine the most favorable orientation of the proximal methyl groups, they were rotated individually and the total energy of the molecule was calculated for each conformer. The results are summarized in Figure 9. The calculations suggest that the orientation of the methyl groups of the pyrazol ring can significantly alter the energy of the process. When the most favorable orientation of the methyl groups is incorporated into the calculation, the energy of activation is reduced to 41.77 kcal/mol. Interestingly, the difference in energy between the two isomers calculated both at the semiempirical and DFT levels is in excellent agreement with that observed from the electrochemical measurements (Figure 3). The influence of the steric interaction between the bulky *tert*-butyl and methyl groups of the L1OH ligand was assessed by calculating the energies of different conformers along the reaction pathway. In these calculations, a truncated model system was used where all bulky groups were omitted (Figure 2). Using this methodology, an activation barrier of 5.3 kcal/mol was estimated, indicating that the steric interaction is the main contributor to the barrier for the twist mechanism. Similarly, a possible dissociative mechanism was also probed by calculating the bond dissociation energies for the Mo−Cl bond at the semiempirical PM3(tm) level (Figure 10).[53] Although the calculated energies are only an estimation, they are slightly higher than those found for the twist mechanism.

As in the usual case, the calculations described above were carried out purely in the gas phase and as such do not account for the solvent effects. One direct consequence of this approximation is that the calculated energy barriers, although comparable to other calculated values, are in poor agreement with experimentally determined energy barriers. Thus, in the absence of other supporting evidence, these calculations cannot be used to determine accurately the relative fitness of either mechanism because of poor resolution of the calculated energies. To probe the possibility of a bond dissociation mechanism, the isomerization reaction has been further investigated in the presence of excess tetraalkylammonium salts. We hypothesized that if the reaction involved the dissociation of the metal−halide bond the addition of large excesses of halides during the cis-to-trans conversion would result in the formation of mixed-halide trans isomers that could be easily detected by mass spectrometry (Figure 11). As has been previously mentioned, only the $[(L1O)Mo^{V}OCl_2]X^-$-type mixed halides were observed in solution when the isomerization reaction was carried out in the presence of excess alkylammonium halides. The significance of this finding is that if the reaction were to proceed via a dissociative mechanism the excess halide should induce the formation of mixed-halide species (e.g., $[(L1O)Mo^{V}OX_2]Cl^-$, $[(L1O)Mo^{V}OXCl]X^-$). It should be noted that mass spectrometry cannot differentiate between linkage isomers (e.g., $[(L1O)MoOCl_2]Br$ and [(L1O)MoOClBr]Cl). Indeed, a peak cluster resulting from [(L1O)MoOClBr]Cl would indicate a breaking of the Mo−Cl bond. If this were the case, one would expect to observe the formation of peaks attributable to the formation of $[(L1O)MoO_2Br]Br$ or [(L1O)MoOClBr]-

(53) Foresman, J. B.; Frisch, A. *Exploring Chemistry with Electronic Structure Methods*; Gaussian, Inc.: Pittsburgh, PA, 1996.

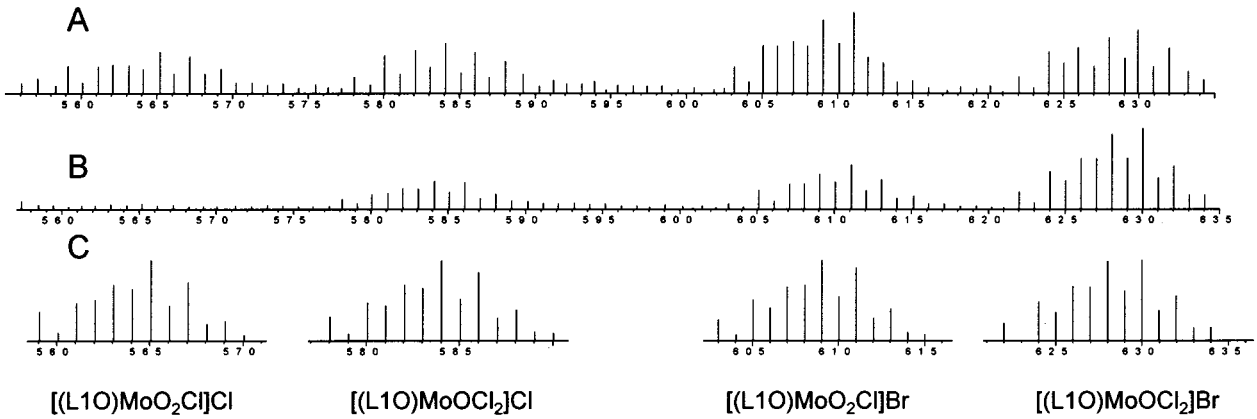

Figure 11. Negative-mode ESI mass spectra of the (A) cis and (B) trans isomers after incubation with a 2-fold excess of Et_4NBr. Calculated isotopic distributions modeling the observed peaks are shown in (C).

Br; however, no such peak was detected. Similar results were also obtained in experiments with excess ^{n}BuNI.

We have already mentioned that both *cis*- and *trans*-(L1O)-$MoOCl_2$ are oxidized under mass spectrometric conditions to generate the dioxo−molybdenum species $(L1O)Mo^{VI}O_2Cl$. Oxidation under mass spectrometric conditions is not uncommon and has been noted earlier.[54] Furthermore, in all cases and under identical conditions, the intensity of the peak cluster due to $[(L1O)Mo^{VI}O_2Cl]X^-$ (X is a halogen) is higher than that of due to $[(L1O)Mo^{V}OCl_2]X^-$ for the cis isomer compared to that for the trans isomer. This observation is in agreement with the electrochemical data.

We are aware that one cannot prove a mechanism; rather, one may only disprove alternative possibilities. In this case, the preponderance of the evidence (i.e., negative entropy, the absence of halide incorporation into the coordination sphere, and quantum chemical calculations) is inconsistent with a dissociative mechanism. Thus, we believe that a twist mechanism is operative in the geometric isomerism.

Implication to the Function of DMSO Reductase. The dependence of the reduction potential on geometry is an important observation, demonstrating that the position of an oxygen donor relative to the terminal oxo functions to modulate the reduction potential of the metal center**.** With respect to the mechanism of the DMSO reductases, this situation leads to the provocative suggestion that the position of the serinato oxygen relative to the terminal oxo may play a critical role in gating the electron-transfer process in the regeneration step. In fact, substrate-bound forms of DMSO reductase exhibit different O_t-Mo-O_{ser} angles compared to the structure with unbound substrate. For example, the O_t-Mo-O_{ser} angle in the DMSO-bound form of the *R. capsulatus* enzyme is 80°, while a much smaller angle is observed for the cacodoic acid-bound form of the *R. sphaeroides* enzyme.[55] Our data suggest that the lower the angle, the easier it is to oxidize Mo(V), while the concomitant reduction becomes more difficult. This geometric flexibility ensures that electron transfer is gated as a function of active-site conformation. We call this proposal the serine-gated electron-transfer hypothesis. The mechanistic investigations reported here suggest that no bond-breaking is necessary for accomplishing such a geometric transformation. A similar kind of geometric alteration with a very low energy barrier has been proposed for the function of xanthine oxidase.[56]

Summary

X-ray crystallography on several DMSO reductases and related enzymes has revealed a variation in the O_t-Mo-O_{ser} angle. Two geometric isomers (*cis*- and *trans*-(L1O)-$MoOCl_2$) have been synthesized to model the physiochemical significance of such a variation on the properties of the enzymes. Both isomers exhibit well-defined reversible oxidation and reduction couples; the reduction of the cis isomer is 216 mV more difficult than the reduction of the trans isomer, while the cis isomer is 135 mV easier to oxidize than is the trans isomer. The electrochemical data are supported by density functional calculations, which suggest an antibonding interaction between the molybdenum d_{xy} orbital and a phenolic oxygen p orbital that raises the energy of the redox orbital. This destabilization makes the cis isomer thermodynamically less stable and allows for spontaneous conversion to the trans isomer. The higher stability of the trans isomer is due to the strong trans influence of the terminal oxo group, which places the bulky ^{t}Bu group in a stereochemically favorable position. A variety of computational and experimental evidence suggests that a twist mechanism is the most likely route for the geometric transformation. On the basis of the results presented here, we propose that a serine-gated electron-transfer process might be important in the catalytic cycle of DMSO reductase and is consistent with the flexibility of the active-site geometry. Our results demonstrate that a delicate balance between the electronic and steric factors is important in determining the relative stability of one isomer over the other. Although the energy barrier measured in the model system may be slightly higher than that in the enzyme, it is conceivable that some degree of fine-tuning of the active-site geometry may lower the energy barrier and thus make the geometric transforma-

(54) Falaras, P.; Mitsopoulou, C.-A.; Argyropoulos, D.; Lyris, E.; Psaroudakis, N.; Vrachnou, E.; Katakis, D. *Inorg. Chem.* **1995**, *34*, 4536.
(55) Schindelin, H. Personal communication.
(56) Jones, R. M.; Inscore, F. E.; Hille, R.; Kirk, M. L. *Inorg. Chem.* **1999**, *38*, 4963.

tion more facile. Additional experiments are underway to further probe this aspect.

Acknowledgment. We thank Professor Hermann Schindelin for providing the coordinates of DMSO reductase prior to publication and Professors Michael Hall, Alastair McEwan, Jeffry Madura, and Martin Kirk for discussions. Financial support to C.J.C. (National Science Foundation, CHE-9726488 and Robert A. Welch Foundation, AI 1157) and P.B. (Hunkele Chateritable Foundation, National Institutes of Health, GM 6155501) is gratefully acknowledged.

Supporting Information Available: Graph showing the energy change associated with the methyl-group rotation, figure containing Eyring and Arrhenius plots is also provided, Table S-I containing kinetic data. This material is available free of charge via the Internet at http://pubs.acs.org.

IC011169W